Programmable Artificial Cells Using Histamine-Responsive Synthetic Riboswitch
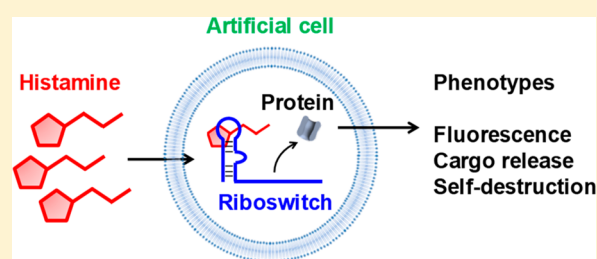
Mohammed Dwidar,[†] Yusuke Seike,[‡] Shungo Kobori,[†] Charles Whitaker,[†] Tomoaki Matsuura,*[‡] and Yohei Yokobayashi*[,†]

[†]Nucleic Acid Chemistry and Engineering Unit, Okinawa Institute of Science and Technology Graduate University, Onna, Okinawa 904-0495, Japan

[‡]Department of Biotechnology, Graduate School of Engineering, Osaka University, 2-1 Yamadaoka, Suita, Osaka 565-0871, Japan

Ⓢ *Supporting Information*

ABSTRACT: Artificial cells that encapsulate DNA-programmable protein expression machinery are emerging as an attractive platform for studying fundamental cellular properties and applications in synthetic biology. However, interfacing these artificial cells with the complex and dynamic chemical environment remains a major and urgent challenge. We demonstrate that the repertoire of molecules that artificial cells respond to can be expanded by synthetic RNA-based gene switches, or riboswitches. We isolated an RNA aptamer that binds histamine with high affinity and specificity and used it to design robust riboswitches that activate protein expression in the presence of histamine. Finally, the riboswitches were incorporated in artificial cells to achieve controlled release of an encapsulated small molecule and to implement a self-destructive kill-switch. Synthetic riboswitches should serve as modular and versatile interfaces to link artificial cell phenotypes with the complex chemical environment.

INTRODUCTION

Artificial cells are cell-like compartments that encapsulate reactive components to mimic cellular behaviors such as replication, metabolism, intercellular communication, and environmental adaptation.[1,2] The compartments can be chemically analogous to those of biological cells such as phospholipid bilayer vesicles and liposomes. Alternatively, synthetic compartments such as polymersomes and colloidosomes have been explored as artificial cell compartments.[3] Similarly, the content of the artificial cells can be enzymes,[4,5] DNA reaction networks,[6] or even living cells.[7] These artificial cells serve as experimental platforms to study cellular behaviors in a constructive (bottom-up) fashion, and as advanced vehicles for applications such as drug delivery and biosensors.[8,9]
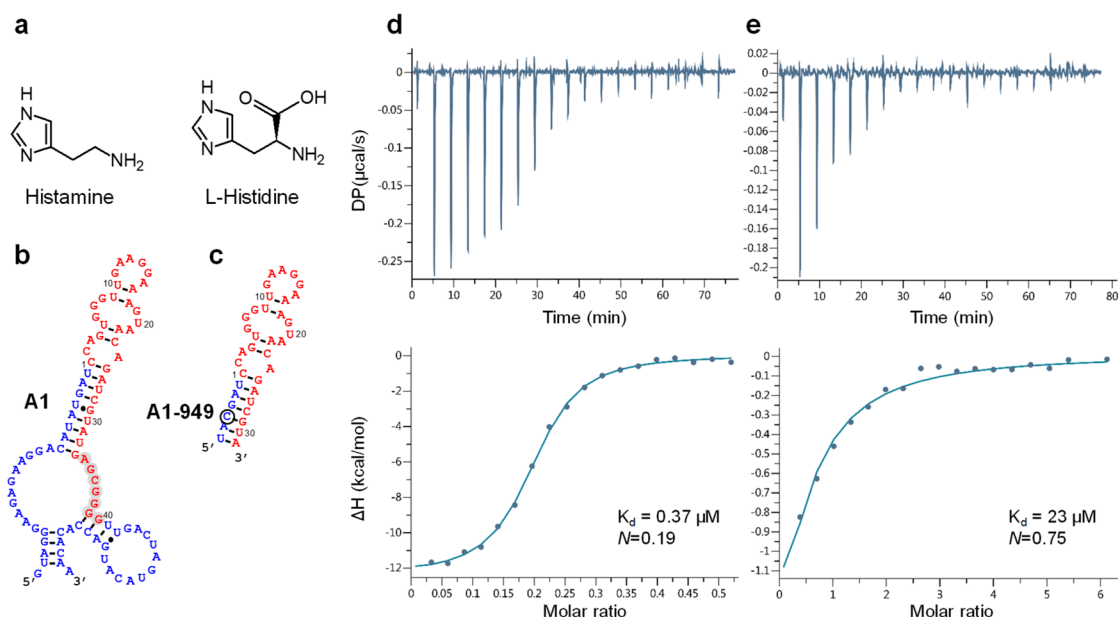
Liposomes encapsulating *in vitro* transcription/translation (IVTT) systems represent artificial cells that mimic the physical compositions and the genetic machinery of natural cells. These artificial cells can use DNA encoded information to express arbitrary proteins inside liposomes.[10−14] Therefore, the potential functions or the phenotypes of this class of artificial cells are limited only by the expressed proteins. However, what is equally or perhaps more important is the ability to control protein expression inside artificial cells. As with natural cells, the ability to regulate gene expression in response to chemical or physical signals is crucial for adaptation of artificial cells to a dynamic environment. Therefore, some efforts to transplant natural mechanisms to control gene expression chemically to artificial cells have been reported, for example, the quorum sensing systems based on acyl homoserine lactone (AHL) signals and their associated transcription factors (TFs),[15−18] as well as other bacterial TFs and their small molecule inducers such as isopropyl β-D-1-thiogalactopyranoside (IPTG), tetracycline, and arabinose.[19,20] However, the use of TF-based gene switches in artificial cells can sometimes be complicated by the need to optimize multiple parameters (amounts of TF and template, promoter design, etc.) carefully, and they have not been engineered to respond to novel chemical signals in artificial cells.

A promising alternative strategy to control gene expression in artificial cells is to use riboswitches. Natural riboswitches control gene expression in bacteria by binding small molecule metabolites and ions in the 5′ UTR of mRNAs and modulating translation efficiency or transcription elongation.[21,22] The wide variety of molecules recognized by RNA aptamers selected *in vitro*[23] offers appealing opportunities for engineering riboswitches that respond to new chemical signals. The lack of protein factors is also favorable for artificial cells that suffer limited protein synthesis capacity. Synthetic riboswitches have been engineered based on natural and synthetic RNA aptamers that bind small molecules to control gene expression in bacteria.[24,25] However, adaptation of riboswitches in artificial cells has been limited. Martini and Mansy[26] first demonstrated the riboswitch function in phospholipid vesicles encapsulating a reconstituted IVTT system (PURE system).[27,28] The

Figure 1. Histamine aptamer. (a) Structures of histamine and L-histidine. (b) Sequence and a predicted secondary structure (by Mfold[34]) of histamine binding aptamer A1. The blue nucleotides are from the constant regions in the RNA library. The red nucleotides represent the selected sequence. The positions found to be highly variable (A34-G40) after reselection are shaded in gray. (c) Sequence and a predicted secondary structure of a truncated aptamer A1-949. The circled cytidine was introduced to stabilize the putative stem structure. (d) ITC measurement of A1-949 binding to histamine. (e) ITC measurement of A1-949 binding to L-histidine. Detailed results of ITC measurements are provided in Table S3.
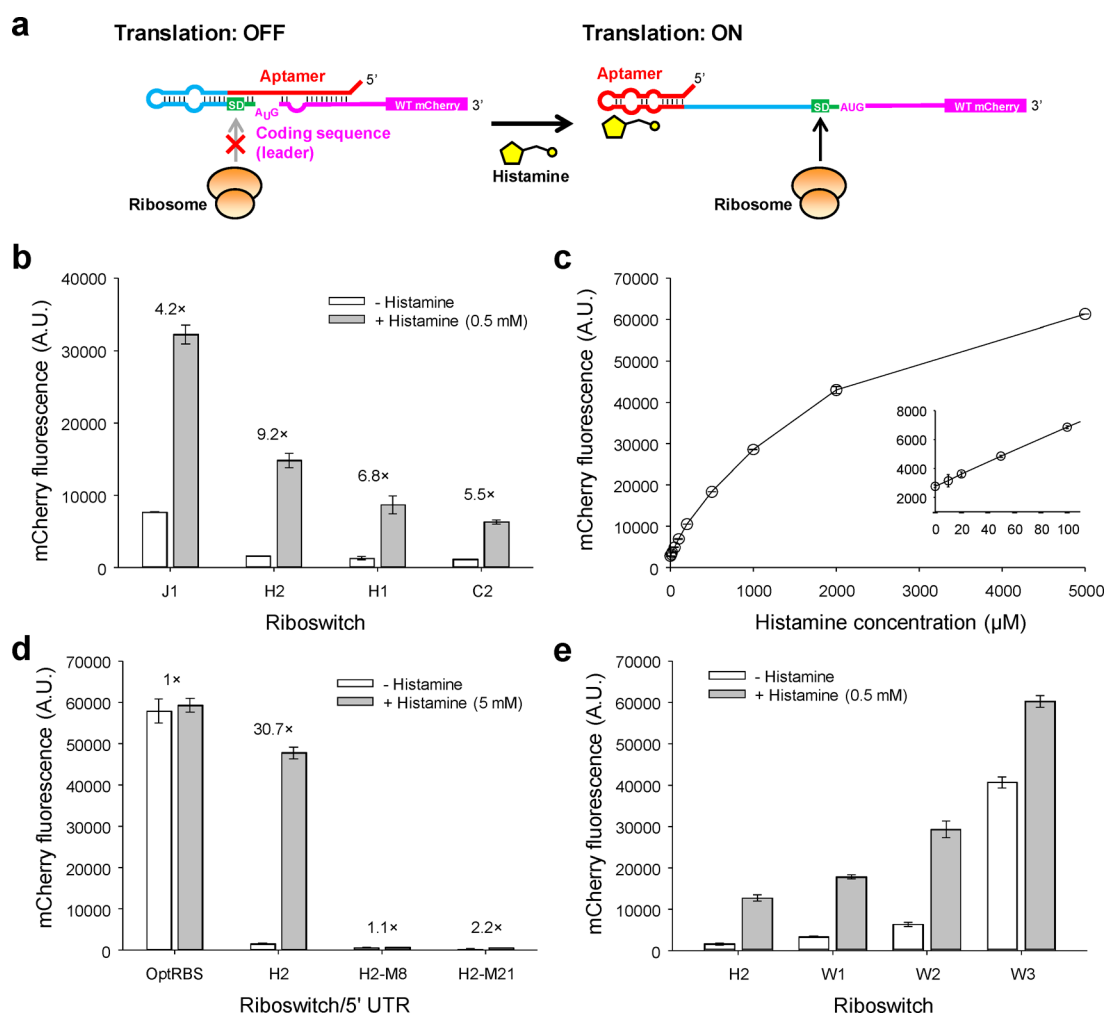
researchers observed ~6-fold activation of a fluorescent reporter protein (YPet) expression in a bulk IVTT system in response to theophylline, but the induced expression level was very low, and the expression level in vesicles was not quantified. Lentini et al.[29] and Adamala et al.[19] later used the theophylline riboswitch to control α-hemolysin (αHL) expression in liposomes to release the coencapsulated IPTG or doxycycline in response to theophylline to control *Escherichia coli* or other artificial cells, respectively. While these reports elegantly demonstrated the potential of riboswitches to engineer chemically responsive artificial cells, the riboswitch performance (ON/OFF ratio and induced expression level) was rather poor, with a reported ON/OFF ratio of ~1.5 in Lentini et al.[29] A similar riboswitch was also used by Adamala et al.,[19] but they did not directly report the riboswitch performance. They observed ~3-fold activation of reporter gene expression in a cascaded gene circuit, which also implicates poor riboswitch performance. Theophylline is also a popular ligand for proof-of-principle riboswitch experiments because it is one of the few small molecule−aptamer combinations that have been shown to function in cells, but there is little, if any, biological or technical significance as a riboswitch ligand. More generally, relatively low ON/OFF ratios and leaky expression (high OFF level) commonly reported for synthetic riboswitches also likely to make their applications in artificial cells more challenging.[30] Consequently, general utility of riboswitches as chemical gene switches in artificial cells has not been demonstrated. More broadly, there is currently a lack of general strategies to interface artificial cells with the complex chemical environment.

To build artificial cells that respond to a biologically significant chemical input by modulating gene expression, an RNA aptamer must first be obtained by *in vitro* selection, or systematic evolution of ligands by exponential enrichment (SELEX).[23] Subsequently, the aptamer needs to be engineered

to function as an effective riboswitch in an IVTT system, and finally encapsulated in vesicles and characterized. Here, we describe the first implementation of this design strategy for artificial cells that genetically respond to a biologically important small molecule for which there are no known TF-based sensors. We chose to sense histamine (Figure 1a), a natural signaling molecule involved in inflammatory response[31] and a neurotransmitter.[32] Histamine is produced by decarboxylation of histidine (Figure 1a), and it is naturally sensed extracellularly through G-protein coupled receptors (GPCRs),[33] which would be difficult to adapt to artificial cells. We isolated a histamine specific aptamer by SELEX, characterized it *in vitro*, and the aptamer was engineered to function as robust riboswitches that induce protein expression in the presence of histamine in a reconstituted IVTT system. Finally, the riboswitch was fused to a reporter gene and other genes, encapsulated in phospholipid vesicles, and the behavior (phenotype) of the artificial cells was quantitatively characterized. The series of experiments reported in this article demonstrates for the first time that artificial cells can be engineered to respond genetically to a small molecule even in the absence of natural sensors adaptable to artificial cells and paves the way for *de novo* design of artificial cells that can sense and genetically respond to diverse chemical signals for various applications.

■ RESULTS

***In Vitro* Selection of Histamine-Binding RNA Aptamers.** A histamine aptamer was selected from a pool of 2×10^{15} RNA molecules containing up to 3×10^{14} unique sequences within the 40-nt randomized region flanked by 21- and 23-nt constant sequences at the 5′ and 3′ ends, respectively (Table S1). As histamine is a small molecule with few functionalities, L-histidine was immobilized on agarose beads via its carboxyl group so that both the imidazole and the amino groups of histamine would be available for the
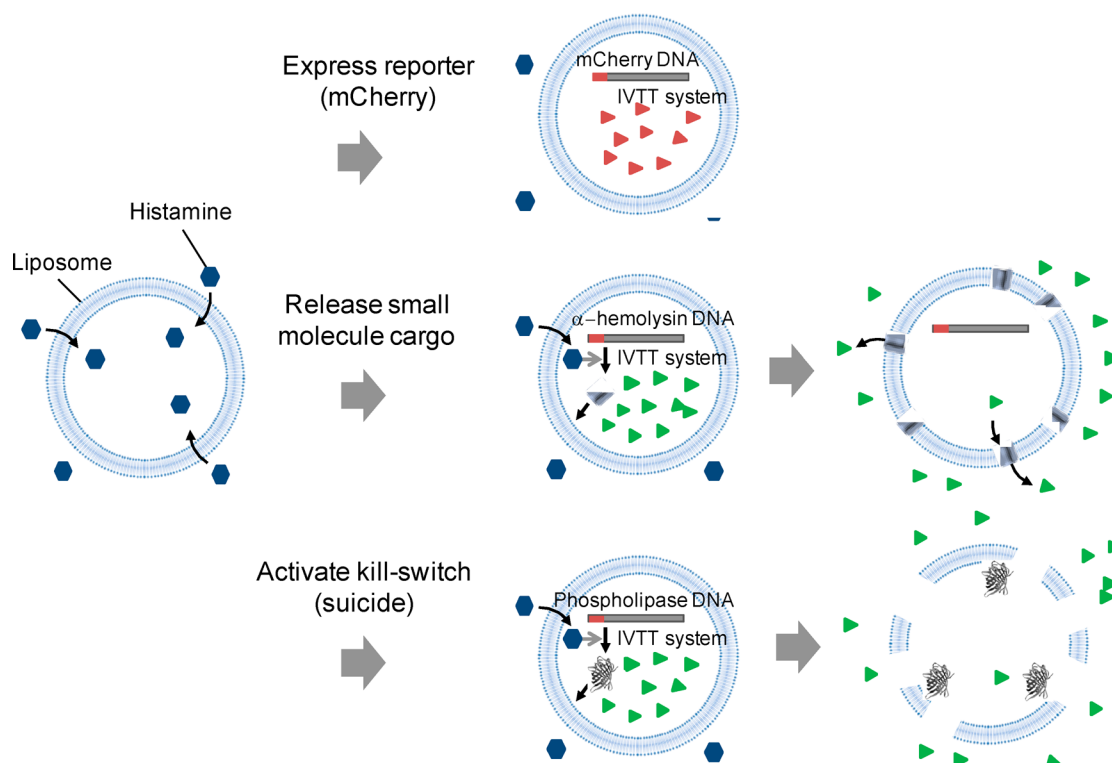
Figure 2. Characterization of histamine riboswitches in IVTT. (a) Riboswitch design strategy. A part of the aptamer was designed to hybridize with the leader peptide sequence in the coding region to sequester the SD sequence and the start codon from the ribosome. Aptamer-histamine binding disrupts the secondary structure and increases the translation efficiency. (b) Screening of riboswitch variants based on the expression of mCherry encoded downstream of each riboswitch. (c) Dose-dependence of the H2 riboswitch. (d) Mutational analysis of the H2 riboswitch in the histamine aptamer. (e) Mutational analysis of the H2 riboswitch to probe the role of the designed stem structure. Sequences of the riboswitch constructs are shown in Figure S5 and Supporting Note 1. (b−d) The samples were measured in duplicates ($n = 2$), and the error bars indicate the range of the two measurements. (e) The samples were measured in triplicates ($n = 3$), and the error bars indicate s.d.

potential aptamers to interact (Figure 1a). Stringency of the selection was gradually increased by additional washing steps, introduction of negative selection against L-histidine (from round 8), and lowering the histamine concentration in the elution buffer (from round 9) (Table S2). RNA populations before rounds 8, 9, and 11 were then analyzed by deep sequencing and compared with RNA eluted from these selection rounds by histamine as well as by L-histidine to identify histamine-specific aptamer candidates.

Careful analysis of the sequencing results (Supporting Data 1) led us to A1 as a particularly promising candidate (Figure 1b). A1 was found to be the second most abundant sequence in the histamine eluent from round 11, constituting 17.2% of the sequenced population. On the other hand, A1 comprised 5.8% of the L-histidine eluent, indicating the preference of A1 to bind histamine. None of the other 12 sequences with abundance >0.5% in the histamine eluent from round 11 showed comparable preference for histamine over L-histidine. Furthermore, the abundance of A1 in the histamine eluent progressively increased from 0.099% in round 8 to 0.33% in round 9, and to 17.2% in round 11. Consequently, the full A1

sequence including the flanking constant regions was synthesized by *in vitro* transcription and characterized by isothermal titration calorimetry (ITC). A1 showed a dissociation constant (K_d) of 0.4 μM for histamine and 47 μM for L-histidine, respectively (Figure S1), confirming its high affinity for histamine and selectivity against L-histidine.

Minimization of A1 Aptamer. To identify the core sequence of the aptamer necessary for histamine binding, a partially randomized library of the A1 aptamer was prepared by doping the selected bases at a rate of 21%. The library was subjected to four rounds of stringent selection for histamine binding (Table S2) and sequenced (Supporting Data 2). The sequences which were enriched more than 50-fold after four rounds of selection were analyzed to determine the variability of each nucleotide in the aptamer sequence (Figure S2). C1 through G33 were generally well conserved with some variability observed at U5, A16, A17, A18, and A26. However, A34 through G40 were highly variable, indicating that these positions are not critical for histamine binding. These observations and the predicted secondary structure of the

Figure 3. Programming artificial cells using a synthetic histamine-responsive riboswitch. By changing the protein whose expression is controlled by the riboswitch, the artificial cells exhibit various phenotypes such as becoming fluorescently active, releasing a low molecular weight compound trapped inside artificial cells, or activating a kill-switch leading to self-destruction, in response to histamine in the environment.

full A1 sequence by Mfold[34] (Figure 1b) led us to A1-949 as a core aptamer sequence (Figure 1c).

ITC measurements of A1-949 yielded dissociation constants (K_d) for histamine (0.37 μM) and L-histidine (23 μM), which are comparable to those of A1 (Figure 1d,e). The stoichiometry (N) was significantly lower than 1.0, which may be due the formation of nonfunctional complexes. Native gel electrophoresis of A1 showed multiple bands (Figure S3) suggesting that the aptamer may form multiple secondary structures or multimeric complexes, therefore lowering the effective aptamer concentration capable of ligand binding. The high RNA concentration (25−50 μM) necessary for accurate ITC measurements further increases the probability of forming intermolecular complexes. Similar deviations from the ideal stoichiometry in small molecule binding RNA aptamers have been reported previously.[35] To support the ITC results, Cy5-labeled A1-949 was chemically synthesized and was used to measure the aptamer affinity by microscale thermophoresis (MST), which yielded K_d values of 1.7 and 362 μM for histamine and L-histidine, respectively (Figure S4). These results confirm the high affinity of A1-949 for histamine and high selectivity against L-histidine.
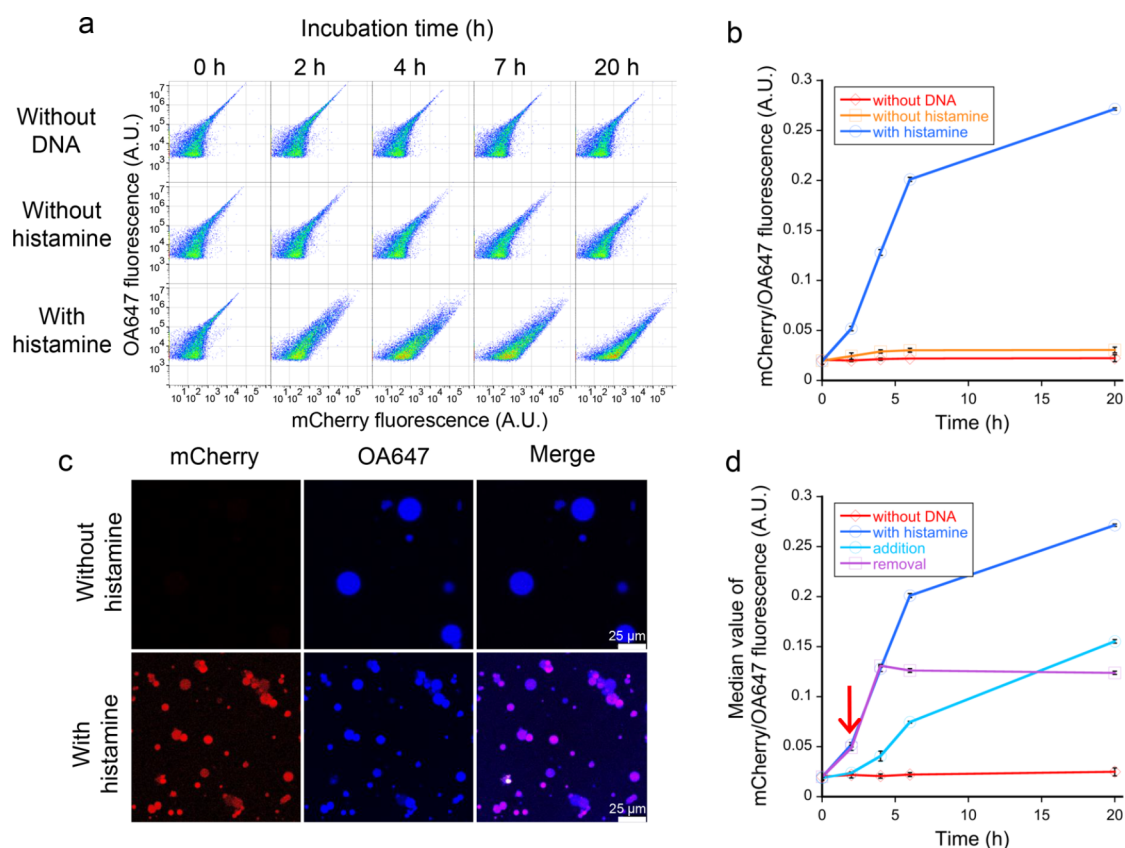
Engineering Histamine-Responsive Riboswitches. With a histamine aptamer in hand, our next aim was to engineer histamine-responsive riboswitches that function in a reconstituted IVTT system. Bacterial riboswitches are typically engineered by screening a large number of "expression platform" sequences between an aptamer and a ribosome binding site (RBS) in bacteria (mostly E. coli) using a reporter gene or a selection marker.[36,37] However, cell-based screening was not a promising strategy for histamine riboswitches because histamine is a polar molecule which is unlikely to

diffuse through the bacterial cell membrane. Furthermore, we deemed it more appropriate to optimize the riboswitch function in the environment in which the riboswitches are intended to be used, namely, the IVTT system that would later be encapsulated in liposomes to create programmable artificial cells. For this purpose, DNA templates encoding the T7 promoter, a riboswitch, and mCherry sequences were constructed (designated T7-[riboswitch]-mCherry) and evaluated using the PURE system[28] (PUREfrex 1.0) for IVTT.

Our riboswitch design strategy was loosely based on the previously described synthetic riboswitches isolated by screening or selection in E. coli.[38,39] These riboswitches form a stable secondary structure in the absence of the ligand that sequesters the Shine-Dalgarno (SD) sequence and the start codon (AUG), thereby translationally repressing protein expression. Aptamer−ligand interaction interferes with this structure, resulting in increased accessibility of the SD sequence and the start codon to the ribosome to activate translation (Figure 2a). A unique feature of our design was to incorporate a leader peptide coding region (∼27 nt including the start codon) that forms a stable stem structure with part of the histamine aptamer (Figure S5). This extra leader peptide was inserted upstream of the native mCherry coding sequence, therefore forming a part of the riboswitch module which needs to be included when regulating another gene.

Riboswitches J1, H1, H2, and C2 (Figure S5, Supporting Note 1) were designed to fold into similar structures using RNAfold server in ViennaRNA Web Services,[40] intended to represent different local structures and stabilities. No attempt was made to predict the secondary structures of the ligand-bound riboswitches, as the accuracy and practical significance of such structures are questionable. The four riboswitch

Figure 4. Histamine-responsive expression of mCherry in artificial cells. (a) The two-dimensional plots show the relationship between OA647 fluorescence intensity, representing the aqueous volume of the liposome, and mCherry fluorescence intensity. (b) Time course of the median value of mCherry/OA647 fluorescence intensity which represents the relative mCherry concentration inside the liposome. The error bars represent the s.e. calculated from 20 000 particle data obtained by FCM. A similar result was observed in the technical repeat experiment (Figure S8a). (c) Confocal imaging of artificial cells with or without histamine exposure. (d) The effect of removal and addition of histamine during mCherry synthesis. Histamine was removed by pelleting the artificial cells by centrifugation and exchanging the supernatant with the buffer without histamine. The arrow indicates the time when histamine was added or removed. The error bars represent the s.e. calculated from 20 000 particle data obtained by FCM. A similar result was observed in the technical repeat experiment (Figure S8b).

candidates were evaluated in the presence (0.5 mM) and absence of histamine (Figure 2b). While all four designs responded to histamine by upregulating mCherry expression, the riboswitch H2 (DNA template T7-H2-mCherry, Supporting Note 1) showed the highest ON/OFF ratio of 9.2. H2 was further characterized under various histamine concentrations (Figure 2c). This robust riboswitch yielded an ON/OFF ratio as high as 30.7 (Figure 2d) albeit at a relatively high histamine concentration (5 mM). It was also confirmed that H2 does not respond to L-histidine, D-histidine, and imidazole (Figure S6).
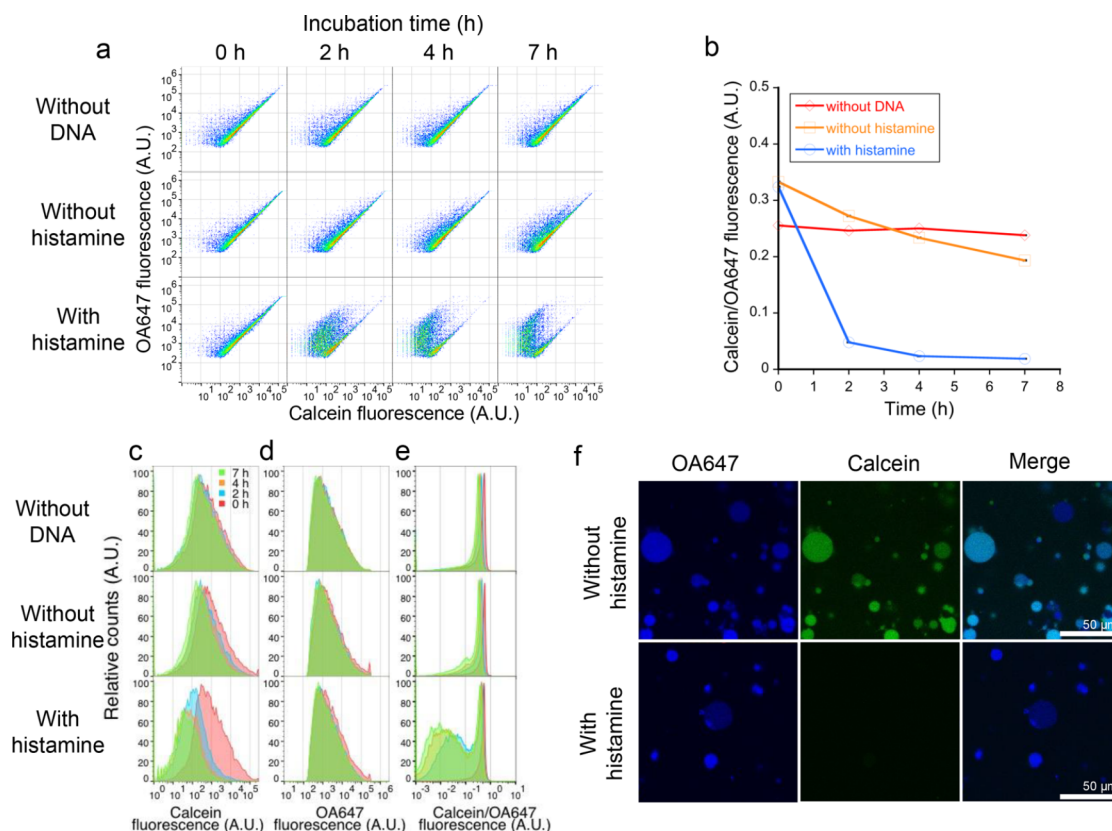
To rule out nonspecific activation of gene expression by histamine, single-base mutations were introduced within the conserved nucleotides in the aptamer in the H2 riboswitch. The mutant riboswitches H2-M8 and H2-M21 (Supporting Note 1) both failed to activate gene expression in the presence of histamine (Figure 2d). Another control construct (OptRBS) lacking the histamine aptamer and harboring an optimal RBS sequence suggested by the RBS Calculator[41] showed strong mCherry expression with or without histamine. These results clearly confirm that the riboswitch function is dependent on the specific interaction between the aptamer and histamine. Moreover, the induced expression level is comparable to that of an efficiently translated mRNA (OptRBS) (Figure 2d). The riboswitches H2 and J1 were also tested in a cell extract-based IVTT system (E. coli S30 Extract, Promega) transcribed from

the *tac* promoter by *E. coli* RNA polymerase (Figure S7) and were confirmed to be functional.

To support further the proposed riboswitch mechanism, we prepared several mutants of H2 in which the stem between a part of the aptamer and the leader coding sequence was progressively weakened. W1 and W2 each contains one mismatch resulting from a single-base, synonymous mutation in the leader peptide region (Figure S5). These mutants showed moderate increases in mCherry expression both in the absence and presence of histamine (Figure 2e). The two mutations were combined in W3, which resulted in a significant degradation of the performance as a switch (Figure 2e).

The robust riboswitches that function in the IVTT system allow us to program the artificial cells to perform various tasks in response to histamine by controlling expression of different proteins. To demonstrate the versatility of riboswitches to program artificial cells, we designed artificial cells that simply express a reporter gene, release small molecule cargo, or self-destruct in response to histamine (Figure 3).

Construction and Characterization of Histamine-Responsive Artificial Cells. We first aimed to investigate whether the artificial cells harboring T7-H2-mCherry can respond to the histamine added to the external solution of artificial cells (Figure 3, top panel). Artificial cells were

Figure 5. Histamine-responsive expression of αHL in artificial cells and selective release of calcein. (a) The two-dimensional plots show the relationship between OA647 fluorescence intensity, representing the aqueous volume of the liposome, and calcein fluorescence intensity. (b) Time course of the median value of calcein/OA647 fluorescence intensity, which represent the relative calcein concentration inside the liposome. The error bars represent the s.e. calculated from 20 000 particle data obtained by FCM. A similar result was observed in the technical repeat experiment (Figure S8c). Histograms of the (c) calcein, (d) OA647, and (e) calcein/OA647 fluorescence of the two-dimensional plots shown in panel a. (f) Confocal images of artificial cells with or without histamine exposure.
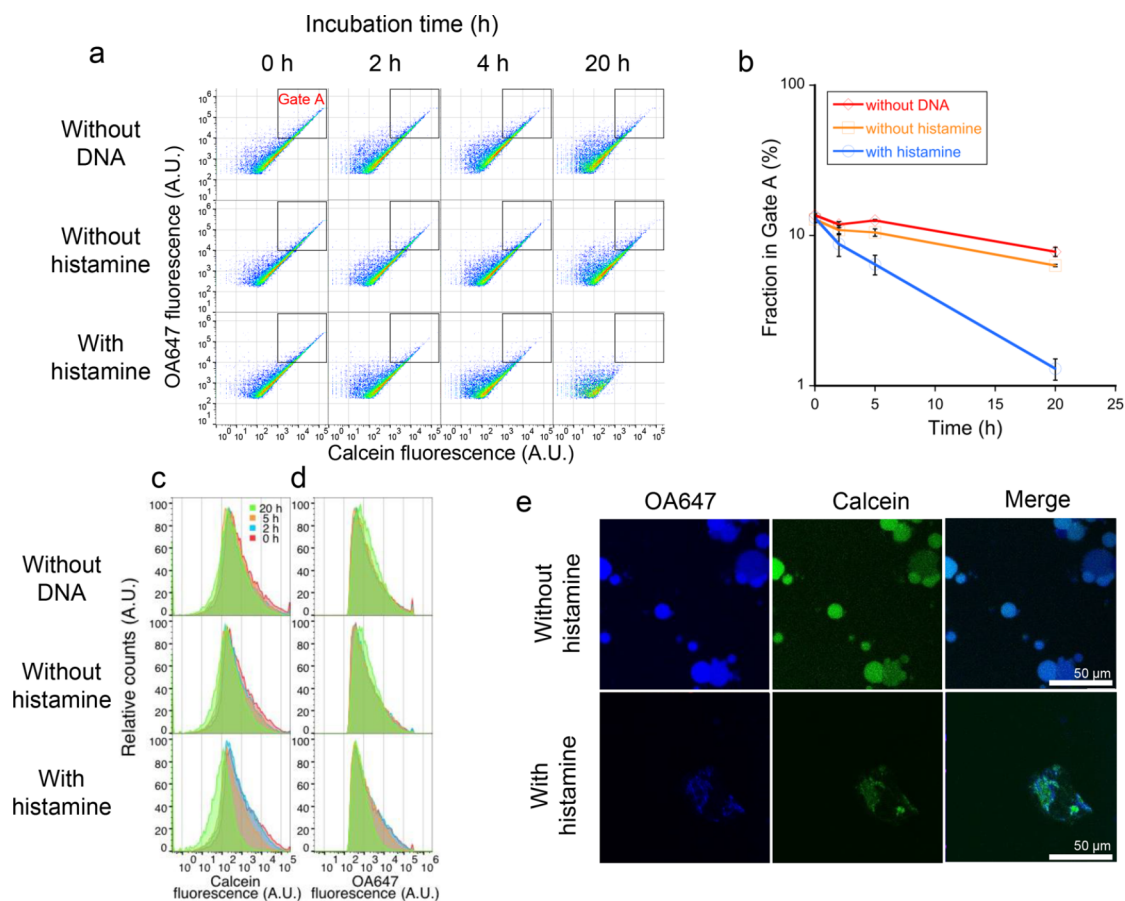
prepared by encapsulating T7-H2-mCherry DNA together with the reconstituted IVTT into the liposome. As a fluorescent protein marker, ovalbumin conjugated to Alexa-Fluor647 (OA647) (45 kDa) was also included to indicate the aqueous volume of the liposomes. Histamine (10 mM) was added to the external solution of the liposomes, incubated at 37 °C to initiate the protein synthesis, and mCherry fluorescence was evaluated using flow cytometry (FCM) and confocal fluorescence microscopy (Figure 4). FCM data showed that mCherry fluorescence of the liposomes increased over time when histamine was present (Figure 4a). T7-H2-mCherry yielded an ON/OFF ratio as high as 30.3 after 20 h of incubation (Figure 4b), a value similar to that obtained in a batch reaction (Figure 2b). Confocal fluorescence imaging showed that mCherry was synthesized and distributed uniformly inside the liposome in the presence of histamine (Figure 4c). These results show that the riboswitch H2 also functions inside liposomes.

To demonstrate the switching ability of protein expression inside the artificial cells, histamine was first added to the external solution of artificial cells and was then removed after 2 h. The mCherry fluorescence increase terminated after 4 h (Figure 4d). The observed delay in the termination is likely due to the slow folding of mCherry,[42] i.e., mCherry synthesis stopped after 2 h incubation but mCherry folding continued for additional 2 h. Conversely, histamine was added for the first time after 2 h incubation at 37 °C. The mCherry fluorescence

hardly increased during the first 2 h, whereas a clear increase was observed after the addition of histamine (Figure 4d). These results clearly demonstrate that histamine is membrane-permeable, and the expression in artificial cells can be dynamically controlled by the addition or removal of histamine.

The FCM analysis revealed that more than 80% of the artificial cells showed detectable mCherry fluorescence in the presence of histamine (Figure S9a). The artificial cells used in this study were prepared using the water-in-oil (W/O) emulsion/transfer method[43] (see Methods for details), and the aqueous volume of cells prepared in this way was reported to be between 1 to 100 fL.[44,45] The template DNA is the IVTT component with the lowest concentration at 5 nM, which corresponds to on average 3 to 300 copies per liposome. This implies that even the smallest artificial cells contain all IVTT components at similar concentrations which is consistent with our observation that the majority of the artificial cells showing detectable mCherry fluorescence in the presence of histamine (Figure S9a).

Controlled Release of Small Molecule Cargo by Artificial Cells. With a robust riboswitch that functions in liposomes in hand, we sought to use the riboswitch to regulate other genes to confer new phenotypes to the artificial cells. First, we used the H2 riboswitch to control an engineered version of the α-hemolysin (αHL)[46] pore-forming protein from *Staphylococcus aureus*. Addition of histamine activates the

Figure 6. Histamine-responsive expression of PLC in artificial cells as a kill-switch. (a) The two-dimensional plots show the relationship between OA647 fluorescence intensity representing the aqueous volume of the liposomes and calcein fluorescence intensity. (b) Time course of the fraction of liposome present in Gate A. Each data point represents mean ± s.e. of three independent measurements. Histograms of (c) calcein and (d) OA647 fluorescence of the two-dimensional plots shown in Figure 6a. (e) Confocal images of artificial cells with or without histamine exposure.

riboswitch to express αHL within the liposomes. The pore-forming αHL proteins are incorporated into the lipid bilayer of the liposomes, which allow diffusion of small molecules less than ~3 kDa across the liposomal membrane, but macromolecules such as proteins remain in the artificial cells (Figure 3, middle panel). In other words, artificial cells can be chemically triggered to release encapsulated small molecules. DNA template T7-H2-αHL was encapsulated in artificial cells along with the reconstituted IVTT mixture, OA647 (45 kDa), and calcein (623 Da). Calcein does not diffuse through lipid bilayer and emits green fluorescence, therefore serving as model small molecule cargo, while OA647 is expected to remain in the liposomes even when αHL is expressed. Histamine (10 mM) was added to the external solution of the liposomes, incubated at 37 °C to initiate the protein synthesis, and the fluorescence was evaluated using FCM and confocal fluorescence microscopy (Figure 5).

The FCM data showed a decrease in calcein fluorescence while that of OA647 remained unchanged during the incubation (Figure 5a,c,d) in the presence of histamine. This result indicates the nanopore formation by αHL. Consequently, a 17-fold decrease in the median value of the relative concentration of calcein inside the liposome was observed (Figure 5b). The FCM data indicate more than 80% of the artificial cells show detectable decrease in calcein fluorescence (Figure S9b). The result was further confirmed by confocal fluorescence imaging where both calcein and OA647

fluorescence was observed in the absence of histamine, whereas the depletion of calcein fluorescence was observed in the presence of histamine (Figure 5e). These results show that the artificial cells can be programmed to release small molecules in response to histamine via the synthetic riboswitch.

Histamine Induced Self-Destruction of Artificial Cells. Self-destruction of artificial cells can also be induced by histamine (Figure 3, bottom panel). DNA encoding the T7 promoter, H2 riboswitch, and phospholipase C (PLC),[47] an enzyme that cleaves phospholipids before the phosphate, was constructed (T7-H2-PLC). Artificial cells were prepared by encapsulating T7-H2-PLC DNA together with the reconstituted IVTT, OA647, and calcein. Histamine (10 mM) was added to the external solution of the liposomes, incubated at 37 °C to initiate the protein synthesis, and the fluorescence was evaluated using FCM and confocal fluorescence microscopy (Figure 6).

The FCM data showed a decrease in the population of liposomes with strong calcein and OA647 fluorescence intensity (Figure 6a) in the presence of histamine. The fraction of liposomes in Gate A showed a much greater decrease in the presence of histamine compared to those without histamine and without T7-H2-PLC (Figure 6b). In addition, fluorescence of both calcein and OA647 decreased during the incubation (Figure 6c,d). The result was also confirmed by confocal fluorescence imaging where both

calcein and OA647 fluorescence was observed in the absence of histamine, whereas the liposomes were hardly detectable and only membrane fragments were observed in the presence of histamine (Figure 6e). These observations are consistent with physical destruction of the artificial cells. We performed similar experiments using phospholipase A1 (PLA1)[48] which cleaves the acyl chain of the phospholipid. In this experiment, the liposomes were prepared using a fluorescently labeled (green) lipid to detect the membrane rupture directly (Figure S10). In the presence of histamine, a decrease in green fluorescence was observed by FCM, again indicating self-destruction of the artificial cells (Figure S10a). These results show that the artificial cells can be programmed to self-destruct (suicide) in response to histamine via the synthetic riboswitch.

■ DISCUSSION

The ability to sense and genetically respond to chemical signals inside and outside of cells is crucial for both natural and artificial cells. However, the current scarcity of genetic devices that can interface artificial cells with the complex chemical environment will likely limit the future applications of artificial cells. Riboswitches have a number of desirable properties as chemical gene switches in artificial cells. First, the well-established technique of *in vitro* selection of RNA aptamers from a pool of random sequences should allow development of RNA aptamers for a variety of chemical signals.[23] Second, development of riboswitches using natural and synthetic RNA aptamers have been reported extensively in bacteria.[24,25] Finally, riboswitches require no protein cofactors that need to be expressed intracellularly or added in pure form. These characteristics should allow engineering of riboswitches that respond to desired chemical signals by expressing arbitrary proteins in artificial cells. In practice, however, only the theophylline riboswitches with modest performance have been used to control gene expression in artificial cells,[19,26,29] and the often-stated promise of riboswitches enabling artificial cells to sense and respond to the complex extra- and intracellular chemical environments has not been substantiated.

The newly isolated histamine aptamer was successfully converted into synthetic riboswitches with high ON/OFF ratios, up to 30.7 and 30.3 in batch and in artificial cells, respectively. Furthermore, induced expression levels (ON level) was nearly identical to the construct with an optimal RBS sequence (and no riboswitch) in a bulk IVTT system (Figure 2). Riboswitches with such high ON/OFF ratios and expression levels are uncommon. However, our riboswitches require ∼1 mM histamine for ∼10-fold activation of gene expression (Figure 2b,c), which is significantly high (histamine concentration) considering the low K_d of the aptamer. Similar discrepancies between the aptamer–ligand affinity and the riboswitch response have been observed in natural and synthetic riboswitches in bacteria,[49,50] which have been attributed to the existence of competing RNA structures and kinetic control. While we opted for few cycles of trial-and-error to discover several robust riboswitches, high-throughput screening methods in IVTT would be desirable to engineer more sensitive riboswitches for artificial cell applications. For example, liposome display technology[46,51] may be used to engineer riboswitches that show superior expression at lower histamine concentrations. Alternatively, genetic circuits such as the positive feedback loop may be used to amplify the riboswitch response.[20] Our histamine riboswitch also functioned in liposomes without further optimization. Histamine

was found to diffuse through the phospholipid bilayer (Figure 4d). For chemical inputs that have lower permeability across artificial cell membrane, modifications such as membrane incorporation of protein pores or transporters may be necessary. A significant improvement in sensitivity is necessary for the riboswitch-engineered artificial cells to sense biologically relevant histamine concentrations; a recent GPCR-based histamine sensor constructed in mammalian cells showed an EC_{50} of ∼100 nM histamine.[52]

Histamine is naturally sensed by the membrane-integrated GPCRs, and it is not known to be membrane permeable. However, histamine was found to penetrate the membrane of the artificial cells passively. We showed that mCherry expression, release of an encapsulated small molecule, and self-destruction occur only when histamine was added to the external solution of the artificial cells (Figures 4−6). Furthermore, addition or removal of histamine to or from the external solution of the artificial cells resulted in initiation or termination of mCherry expression, respectively (Figure 4d). This observed switching behavior of the riboswitch-containing artificial cells clearly demonstrates that histamine diffuses through the artificial cell membrane. Similarly, many amino acids have been shown to permeate the artificial cell membrane,[53] while natural cells use transporters to transport amino acids. The natural and artificial cells have significant differences in the membrane structure. Artificial cell membrane used in this study is composed of purified phosphatidylcholine and cholesterol, while that of the natural cells consist of various phospholipids, integral membrane proteins, and lipid associated proteins. The lack of such complex structures in artificial cells is likely to have affected the membrane permeability of histamine.

The riboswitches, through the aptamer domain, offer opportunities to interface artificial cells with numerous intra- or extracellular chemical signals. The output of the interface is (conditional) expression of arbitrary proteins which also opens the door to many possible outcomes (phenotypes) (Figure 3). In this work, in addition to fluorescent protein expression (Figure 4), we demonstrated conditional release of a small molecule (calcein) trapped inside artificial cells via riboswitch-activated expression of αHL. Other canonical gene switches have been used to control αHL expression in liposomes.[18,19,29] While these earlier studies demonstrated the use of αHL to release small molecules encapsulated in artificial cells, the process was not thoroughly characterized. For example, while Tang et al. measured the dequenching of the released calcein in the outer bulk solution,[18] we directly measured the fluorescence distribution of the artificial cells by FCM. Similarly, the release of entrapped IPTG through αHL was indirectly monitored by the activation of GFP expression in cocultured *E. coli* by Lentini et al.,[29] and the released doxycycline was indirectly detected by reporter gene expression in other artificial cells by Adamala et al.[19] In this work, we directly and quantitatively observed the controlled release of a small-molecule compound (but not proteins) encapsulated in artificial cells in the presence of histamine by fluorescence microscopy and FCM (Figure 5), observing about a 20-fold decrease in the calcein concentration upon riboswitch activation.

Robust chemically controlled release of molecular cargo may be useful for drug delivery and other applications. Histamine is released by mast cells and basophils in response to antigen exposure.[31] A possible future direction is to program artificial

cells to respond to histamine released by mammalian cells by delivering antihistamine or anti-inflammatory drugs. We demonstrated another phenotype by fusing the riboswitch to a gene encoding PLC (Figure 6) and PLA1 (Figure S10). By catalyzing phospholipid hydrolysis, phospholipase expression was expected to result in disintegration of the artificial cells. We envisioned it as a model of a "kill-switch" which can be used to program artificial cells to self-destruct after their intended tasks are completed, or when they result in undesirable or unexpected consequences and need to be shut down. As expected, activation of phospholipase expression resulted in degradation of the artificial cells as observed by FCM and fluorescence microscopy (Figure 6, Figure S10). Taken together, these results support the modularity of riboswitches to control expression of arbitrary proteins in response to an aptamer ligand, thereby greatly expanding the potential phenotypes that can be controlled by chemical signals. However, such practical applications of chemically responsive artificial cells will need to overcome various technical challenges, for example, long-term stability of the artificial cells, and toxicity and immunogenicity of the expressed proteins. Because riboswitches function inside artificial cells, additional protein devices such as transporters or pore-forming membrane proteins may be necessary to sense molecules that do not efficiently diffuse across lipid bilayers using riboswitches.

In conclusion, we addressed one of the significant and imminent challenges for artificial cell research and applications, namely, to interface them with the complex and diverse chemical signals. We demonstrated the possibilities of riboswitches as a promising chemical interface to connect arbitrary chemical signals (via developing new RNA aptamers) with arbitrary genetic output (proteins) to program artificial cells.

■ METHODS

Oligonucleotides and Molecular Biology Reagents. A DNA library with 40 degenerate bases flanked by constant sequences (tempN40) and the primers (RevSel and T7-prom-fwd) for reverse transcription and polymerase chain reaction (PCR) during SELEX were purchased from Trilink Biotechnologies (Table S1). Partially randomized DNA based on the A1 aptamer sequence (RC-temp-A1-doped) was synthesized by GeneDesign and contained 79% original (A1 aptamer) base mixed with 7% each of the remaining three bases (Table S1). OneTaq 2X Master Mix (NEB) and Q5 High-Fidelity 2X Master Mix (NEB) were used for PCR in SELEX and sequencing library preparation, respectively. Reverse transcription reactions were performed using Maxima H Minus Reverse Transcriptase (Thermo Scientific). HiScribe T7 Quick High Yield RNA Synthesis Kit (NEB) was used for in vitro transcription of the RNA pool for the first SELEX round, and T7 RNA polymerase (NEB) was used for the subsequent rounds.

Immobilization of Histidine on Agarose Beads. To make both the imidazole and amino groups of histamine available for aptamers to bind, L-histidine was immobilized via its carboxyl group. EAH Sepharose 4B (GE Healthcare) bearing amino groups was employed as an immobilization matrix. Fmoc-L-histidine (Watanabe Chemical Industry) was coupled to the matrix as previously described.[54] Briefly, 10 mL of EAH Sepharose 4B was transferred to a PD-10 column (GE Healthcare) and washed twice with 5 mL of N,N-dimethylformamide (DMF) (Nacalai). The matrix was suspended in 5 mL of DMF containing 30 μmol of Fmoc-L-histidine and 30 μmol of benzotriazol-1-yl-oxytripyrrolidinophosphonium hexafluorophosphate (PyBOP) (Watanabe Chemical Industry). A total of 500 μmol of diisopropylethlamine (DIPEA) (Nacalai) was slowly added while stirring, and the reaction was allowed to proceed for 2 h

at 24 °C. After washing the matrix with DMF (2× 5 mL), it was incubated for 30 min with 5 mL of DMF containing 2 mmol of acetic anhydride (Nacalai) and 2 mmol DIPEA to block the unreacted amino groups on the beads. After washing the matrix with DMF (4× 5 mL), it was treated twice with 5 mL of 20% piperidine (Nacalai) in DMF for 10 min to remove the Fmoc group. The eluents from the two piperidine treatments were combined and the absorbance of the solution at 301 nm ($\varepsilon_M = 9700$)[54] was measured using 20% piperidine in DMF as a blank to determine the amount of the released Fmoc to calculate the coupling efficiency. It was determined that 14.2 μmol of histidine was coupled, which corresponds to approximately 19% of the amino groups on the matrix. The counterselection matrix was prepared in parallel using the same method except in the absence of L-histidine.

SELEX Procedure. The DNA library template tempN40 (0.5 nmol, 3×10^{14} molecules) and RevSel (1 nmol) were mixed in a total volume of 1.5 mL using OneTaq 2X Master Mix (NEB). The mixture was denatured at 94 °C for 4 min followed by four cycles of 94, 48, and 68 °C for 30 s each. Subsequently, 2 nmol of T7-prom-fwd was added and four additional thermal cycles were performed to generate the template for in vitro transcription. The template DNA was column purified (DNA Clean & Concentrator-5, Zymo Research), and 20 μg was used for an overnight RNA transcription reaction in 270 μL volume using HiScribe T7 High Yield RNA Synthesis Kit (NEB). The RNA solution (250 μL) was then mixed with 125 μL of 10× DNase I buffer and treated with 20 U of DNase I (NEB) in a total volume of 1250 μL for 1 h at 37 °C. The RNA was then recovered by ethanol precipitation.

The random RNA pool (110 μg corresponding to approximately 2.3×10^{15} molecules) was dissolved in 2.5 mL of the selection buffer (50 mM HEPES pH 7.0, 250 mM NaCl, and 2 mM glycine), heated to 70 °C for 10 min, and slowly cooled to room temperature. The RNA solution was then supplemented with MgCl$_2$ (5 mM) and CaCl$_2$ (5 mM). The RNA library was incubated with 500 μL of the L-histidine-coupled Sepharose matrix in a PD-10 column for 1 h at 37 °C. The unbound RNA molecules were washed once using 0.5 mL of the selection buffer (with MgCl$_2$ and CaCl$_2$), and the bound sequences were eluted using 2× 1 mL of the selection buffer (with MgCl$_2$ and CaCl$_2$) containing 10 mM histamine. The eluted RNA molecules were then ethanol precipitated after the addition of Quick-Precip Plus Solution (EdgeBio). The recovered RNA pool was reverse transcribed, PCR amplified, and in vitro transcribed to produce the RNA pool for the second round. Starting from the second round, 1.5 μg of RNA dissolved in 2 mL of selection buffer was applied to the matrix, and each cycle was preceded with a counterselection in 500 μL of the acetylated matrix. Starting from the fourth round, mutagenic PCR was performed to increase the diversity of the library.[55] A negative selection step using L-histidine was also included from round 8. Histamine concentration during the elution step was reduced to 0.2 mM in rounds 9−11. From round 4, CaCl$_2$ was removed from the buffer and MgCl$_2$ concentration was gradually reduced. Other selection conditions for each round are summarized in Table S2.

Three columns were used in rounds 8, 9, and 11 for SELEX and to prepare sequencing samples. One column was used for regular SELEX with a negative selection using L-histidine and eluted with histamine. The resulting RNAs were used for the subsequent round of SELEX. The second column was used to perform the same SELEX procedure, but the bound RNA was eluted with histidine (0.2 mM) after the buffer wash step. The third column was similarly eluted with histamine (0.2 mM) after the buffer wash without a negative selection step using histidine. The latter two eluents and the RNA pool before selection from these rounds were separately reverse transcribed and PCR amplified to attach barcodes adapter sequences for deep sequencing. The sequencing samples were analyzed by Illumina MiSeq DNA sequencer using MiSeq Reagent Kit v3. Sequences with more than 10 reads in the histamine elution from round 11 were compiled and shown in Supporting Data 1.

Reselection of Partially Randomized A1 Aptamer. A doped RNA library based on the A1 aptamer selected from the random RNA pool was prepared by annealing and extending oligonucleotides T7-

prom-fwd and RC-temp-A1-doped (Table S1). The selection buffer contained HEPES (50 mM, pH 7.0), NaCl (250 mM), MgCl$_2$ (0.1 mM), and glycine (2 mM). The procedure was similar to the original selection with the following exceptions. The first round was performed using 100 μg of RNA dissolved in 6 mL, and the subsequent rounds were performed using 10 μg of RNA in 2 mL. More stringent histidine negative selections were performed, starting with 1 mM in the first round and 50 mM in the fourth round. Detailed selection conditions are summarized in Table S2. The initial RNA library before SELEX and the eluted RNA pools after each round were analyzed by deep sequencing as described above. Sequences with more than five reads in the final round of the selection were compiled and summarized in Supporting Data 2.

Isothermal Titration Calorimetry (ITC). Both the A1 aptamer and the minimized A1-949 aptamer were transcribed *in vitro* using the HiScribe T7 Quick High Yield RNA Synthesis Kit (NEB) according to the manufacturer's instructions and treated by DNase I. The RNA solutions were treated with phenol/chloroform and precipitated with ethanol. The aptamers were dissolved in the buffer used in SELEX and concentrated using 4 mL Amicon Ultra Centrifugal Filters (Merck) with a 3 kDa cutoff to remove any remaining truncated transcripts and nucleotides. ITC measurements were performed using MicroCal PEAQ-ITC (Malvern). The RNA aptamer was added in the cell while the ligand (histamine or L-histidine) was titrated from the syringe. The cell temperature was maintained at 25 °C. Control reactions in which the ligand was titrated against the buffer, the buffer was titrated against the RNA solution, and the buffer was titrated against the buffer were also performed and used to correct the baseline.

Microscale Thermophoresis (MST). A1-949 (Figure 1c) modified with Cy5 at the 5′ terminus (Cy5-A1-949) was synthesized and high performance liquid chromatography purified by FASMAC. The binding for both histamine and L-histidine was measured using the same buffer used for the SELEX at 25 °C. The experiment was performed by 2bind GmbH.

Riboswitch Design and Evaluation in IVTT System. The mCherry coding sequence was PCR amplified from plasmid Psup-1753-mCherry,[56] and PLC and PLA1 sequences were synthesized by IDT according to the published sequences.[47,48] Riboswitches were designed semirationally with the aid of *RNAfold* server in ViennaRNA Web Services.[40] The DNA templates encoding the T7 promoter, a riboswitch, and a gene of interest were cloned in a plasmid vector and sequence verified. The plasmids were then used as templates in PCR to generate linear DNA templates (Supporting Note 1) for IVTT. IVTT reactions were performed using PURE*frex* 1.0 (GeneFrontier) at a 10 μL volume containing 120 ng of a DNA template and an appropriate concentration of histamine. The solutions were incubated for 4 h at 37 °C in a thermal cycler (Bio-Rad T100), and 8 μL aliquots were transferred to a low-volume 384-well plate. mCherry fluorescence (587 nm excitation/610 nm emission) was measured in a Tecan M1000PRO microplate reader.

Protein Synthesis Inside Liposomes. DNA templates used for IVTT inside liposomes were T7-H2-mCherry, T7-H2-αHL, T7-H2-PLA1, and T7-H2-PLC (Supporting Note 1). Liposomes containing a reconstituted IVTT (PURE*frex*1.0 or 2.0) were prepared using the water-in-oil (W/O) emulsion/transfer method[43] as previously described.[44,45] PURE*frex*1.0 was used for mCherry and PLA1 synthesis and PURE*frex*2.0 was used for αHL and PLC synthesis. Briefly, 20 μL of reconstituted IVTT was supplemented with 5 nM (mCherry and αHL) or 3 nM (PLC and PLA1) template DNA, 400 mM sucrose, 250 mM potassium glutamate, 0.8 U/μL RNase inhibitor, and 1.5 μM ovalbumin Alexa Fluor 647 conjugate (OA647, Thermo Fisher). When necessary, 5 μM calcein was added. In addition, 0.5 mM CaCl$_2$ was added when synthesizing PLA1 or PLC. To this, IVTT solution, 200 μL of liquid paraffin (Wako) containing 0.77 mg of egg phosphatidylcholine (egg PC) (NOF Co.) and 0.77 mg of cholesterol (chol) (Sigma-Aldrich) were added. When labeling the membrane with fluorescence, 0.2 mg of β-BODIPY[R]-FL-C12-HPC (2-(4,4-difluoro-5,7-dimethyl-4-bora-3a,4a-diaza-*s*-indacene-3-dodecanoyl)-1-hexadecanoyl-*sn*-glycero-3-phosphocholine) was

added. The mixtures were vortexed for 30 s to form W/O emulsions that were then equilibrated on ice for 10 min. The solution was gently placed on top of 200 μL of the outer solution (see below for the composition) and centrifuged at 15,000 *g* for 30 min at 4 °C. The pelleted liposomes were collected through an opening at the bottom of the tube. Proteins were synthesized by incubating the liposomes at 37 °C. The outer solution contained the low-molecular weight components of reconstituted IVTT (0.3 mM each amino acid, 3 mM ATP, 3 mM GTP, 1 mM CTP and UTP, 2 mM spermidine, 20 mM creatine phosphate, 2 mM dithiothreitol (DTT), 0.02 μg/μL 10-formyl-5,6,7,8-tetrahydrofolic acid, 250 mM potassium glutamate, 18 mM Mg(OAc)$_2$, 400 mM glucose and 200 mM HEPES (pH 7.6)).

FCM Analysis and Confocal Microscopy. The liposomes were analyzed by FCM using a CytoFlexS (Beckman Coulter, Fullerton, CA) or FACSVerse; (BD). Before FCM analysis, the liposome suspension was diluted 40-fold or 80-fold in a dilution buffer (20 mM HEPES-KOH (pH 7.6), 250 mM potassium glutamate, 18 mM Mg(OAc)$_2$, and 400 mM glucose). A total of 20 000 liposomes were measured. Fluorescence images of the liposome membrane were obtained using a confocal laser scanning microscope (TCS SP8, Leica Microsystems) and a 100× oil immersion objective.

■ ASSOCIATED CONTENT

Ⓢ Supporting Information

The Supporting Information is available free of charge on the ACS Publications website at DOI: 10.1021/jacs.9b03300.

Supporting Figures, Tables, Note (PDF)
Supporting Data 1 (XLSX)
Supporting Data 2 (XLSX)

■ AUTHOR INFORMATION

Corresponding Authors
*yohei.yokobayashi@oist.jp
*matsuura_tomoaki@bio.eng.osaka-u.ac.jp
ORCID Ⓞ
Mohammed Dwidar: 0000-0003-1366-0393
Shungo Kobori: 0000-0003-4995-5847
Tomoaki Matsuura: 0000-0003-1015-6781
Yohei Yokobayashi: 0000-0002-2417-1934

Notes

The authors declare the following competing financial interest(s): Y.Y. and M.D. have applied for a provisional patent on the histamine aptamer and its applications.

■ ACKNOWLEDGMENTS

■ REFERENCES

(1) Buddingh, B. C.; van Hest, J. C. M. Artificial Cells: Synthetic Compartments with Life-like Functionality and Adaptivity. *Acc. Chem. Res.* **2017**, *50*, 769−777.
(2) Lentini, R.; Yeh Martin, N.; Mansy, S. S. Communicating artificial cells. *Curr. Opin. Chem. Biol.* **2016**, *34*, 53−61.
(3) Li, M.; Huang, X.; Tang, T. Y.; Mann, S. Synthetic cellularity based on non-lipid micro-compartments and protocol models. *Curr. Opin. Chem. Biol.* **2014**, *22*, 1−11.

(4) Fujiwara, K.; Adachi, T.; Doi, N. Artificial Cell Fermentation as a Platform for Highly Efficient Cascade Conversion. *ACS Synth. Biol.* **2018**, *7*, 363−370.

(5) Hindley, J. W.; Elani, Y.; McGilvery, C. M.; Ali, S.; Bevan, C. L.; Law, R. V.; Ces, O. Light-triggered enzymatic reactions in nested vesicle reactors. *Nat. Commun.* **2018**, *9*, 1093.

(6) Lyu, Y.; Wu, C.; Heinke, C.; Han, D.; Cai, R.; Teng, I. T.; Liu, Y.; Liu, H.; Zhang, X.; Liu, Q.; Tan, W. Constructing Smart Protocells with Built-In DNA Computational Core to Eliminate Exogenous Challenge. *J. Am. Chem. Soc.* **2018**, *140*, 6912−6920.

(7) Elani, Y.; Trantidou, T.; Wylie, D.; Dekker, L.; Polizzi, K.; Law, R. V.; Ces, O. Constructing vesicle-based artificial cells with embedded living cells as organelle-like modules. *Sci. Rep.* **2018**, *8*, 4564.

(8) Bottom-up biology. *Nature* **2018**, *563*, 171,.

(9) Schwille, P. Bottom-up synthetic biology: engineering in a tinkerer's world. *Science* **2011**, *333*, 1252−1254.

(10) Kita, H.; Matsuura, T.; Sunami, T.; Hosoda, K.; Ichihashi, N.; Tsukada, K.; Urabe, I.; Yomo, T. Replication of genetic information with self-encoded replicase in liposomes. *ChemBioChem* **2008**, *9*, 2403−2410.

(11) Noireaux, V.; Libchaber, A. A vesicle bioreactor as a step toward an artificial cell assembly. *Proc. Natl. Acad. Sci. U. S. A.* **2004**, *101*, 17669−17674.

(12) Nomura, S. M.; Tsumoto, K.; Hamada, T.; Akiyoshi, K.; Nakatani, Y.; Yoshikawa, K. Gene expression within cell-sized lipid vesicles. *ChemBioChem* **2003**, *4*, 1172−1175.

(13) Murtas, G.; Kuruma, Y.; Bianchini, P.; Diaspro, A.; Luisi, P. L. Protein synthesis in liposomes with a minimal set of enzymes. *Biochem. Biophys. Res. Commun.* **2007**, *363*, 12−17.

(14) van Nies, P.; Westerlaken, I.; Blanken, D.; Salas, M.; Mencia, M.; Danelon, C. Self-replication of DNA by its encoded proteins in liposome-based synthetic cells. *Nat. Commun.* **2018**, *9*, 1583.

(15) Ding, Y.; Contreras-Llano, L. E.; Morris, E.; Mao, M.; Tan, C. Minimizing Context Dependency of Gene Networks Using Artificial Cells. *ACS Appl. Mater. Interfaces* **2018**, *10*, 30137−30146.

(16) Lentini, R.; Martin, N. Y.; Forlin, M.; Belmonte, L.; Fontana, J.; Cornella, M.; Martini, L.; Tamburini, S.; Bentley, W. E.; Jousson, O.; Mansy, S. S. Two-Way Chemical Communication between Artificial and Natural Cells. *ACS Cent. Sci.* **2017**, *3*, 117−123.

(17) Rampioni, G.; D'Angelo, F.; Messina, M.; Zennaro, A.; Kuruma, Y.; Tofani, D.; Leoni, L.; Stano, P. Synthetic cells produce a quorum sensing chemical signal perceived by Pseudomonas aeruginosa. *Chem. Commun.* **2018**, *54*, 2090−2093.

(18) Tang, T. D.; Cecchi, D.; Fracasso, G.; Accardi, D.; Coutable-Pennarun, A.; Mansy, S. S.; Perriman, A. W.; Anderson, J. L. R.; Mann, S. Gene-Mediated Chemical Communication in Synthetic Protocell Communities. *ACS Synth. Biol.* **2018**, *7*, 339−346.

(19) Adamala, K. P.; Martin-Alarcon, D. A.; Guthrie-Honea, K. R.; Boyden, E. S. Engineering genetic circuit interactions within and between synthetic minimal cells. *Nat. Chem.* **2017**, *9*, 431−439.

(20) Kobori, S.; Ichihashi, N.; Kazuta, Y.; Yomo, T. A controllable gene expression system in liposomes that includes a positive feedback loop. *Mol. BioSyst.* **2013**, *9*, 1282−1285.

(21) Serganov, A.; Nudler, E. A decade of riboswitches. *Cell* **2013**, *152*, 17−24.

(22) Breaker, R. R. Prospects for riboswitch discovery and analysis. *Mol. Cell* **2011**, *43*, 867−879.

(23) McKeague, M.; DeRosa, M. C. Challenges and opportunities for small molecule aptamer development. *J. Nucleic Acids* **2012**, *2012*, 748913.

(24) Berens, C.; Suess, B. Riboswitch engineering - making the all-important second and third steps. *Curr. Opin. Biotechnol.* **2015**, *31*, 10−15.

(25) Hallberg, Z. F.; Su, Y.; Kitto, R. Z.; Hammond, M. C. Engineering and In Vivo Applications of Riboswitches. *Annu. Rev. Biochem.* **2017**, *86*, 515−539.

(26) Martini, L.; Mansy, S. S. Cell-like systems with riboswitch controlled gene expression. *Chem. Commun.* **2011**, *47*, 10734−10736.

(27) Shimizu, Y.; Inoue, A.; Tomari, Y.; Suzuki, T.; Yokogawa, T.; Nishikawa, K.; Ueda, T. Cell-free translation reconstituted with purified components. *Nat. Biotechnol.* **2001**, *19*, 751−755.

(28) Shimizu, Y.; Kanamori, T.; Ueda, T. Protein synthesis by pure translation systems. *Methods* **2005**, *36*, 299−304.

(29) Lentini, R.; Santero, S. P.; Chizzolini, F.; Cecchi, D.; Fontana, J.; Marchioretto, M.; Del Bianco, C.; Terrell, J. L.; Spencer, A. C.; Martini, L.; Forlin, M.; Assfalg, M.; Dalla Serra, M.; Bentley, W. E.; Mansy, S. S. Integrating artificial with natural cells to translate chemical messages that direct E. coli behaviour. *Nat. Commun.* **2014**, *5*, 4012.

(30) Kobori, S.; Ichihashi, N.; Kazuta, Y.; Matsuura, T.; Yomo, T. Kinetic analysis of aptazyme-regulated gene expression in a cell-free translation system: modeling of ligand-dependent and -independent expression. *RNA* **2012**, *18*, 1458−1465.

(31) Branco, A.; Yoshikawa, F. S. Y.; Pietrobon, A. J.; Sato, M. N. Role of Histamine in Modulating the Immune Response and Inflammation. *Mediators Inflamm.* **2018**, *2018*, 9524075.

(32) Haas, H. L.; Sergeeva, O. A.; Selbach, O. Histamine in the nervous system. *Physiol. Rev.* **2008**, *88*, 1183−1241.

(33) Parsons, M. E.; Ganellin, C. R. Histamine and its receptors. *Br. J. Pharmacol.* **2006**, *147* (Suppl. 1), S127−S135.

(34) Zuker, M. Mfold web server for nucleic acid folding and hybridization prediction. *Nucleic Acids Res.* **2003**, *31*, 3406−3415.

(35) Wu, M. C.; Lowe, P. T.; Robinson, C. J.; Vincent, H. A.; Dixon, N.; Leigh, J.; Micklefield, J. Rational Re-engineering of a Transcriptional Silencing PreQ1 Riboswitch. *J. Am. Chem. Soc.* **2015**, *137*, 9015−9021.

(36) Nomura, Y.; Yokobayashi, Y. Dual genetic selection of synthetic riboswitches in Escherichia coli. *Methods Mol. Biol.* **2014**, *1111*, 131−140.

(37) Rehm, C.; Hartig, J. S. In vivo screening for aptazyme-based bacterial riboswitches. *Methods Mol. Biol.* **2014**, *1111*, 237−249.

(38) Lynch, S. A.; Desai, S. K.; Sajja, H. K.; Gallivan, J. P. A high-throughput screen for synthetic riboswitches reveals mechanistic insights into their function. *Chem. Biol.* **2007**, *14*, 173−184.

(39) Nomura, Y.; Yokobayashi, Y. Reengineering a natural riboswitch by dual genetic selection. *J. Am. Chem. Soc.* **2007**, *129*, 13814−13815.

(40) Gruber, A. R.; Bernhart, S. H.; Lorenz, R. The ViennaRNA web services. *Methods Mol. Biol.* **2015**, *1269*, 307−326.

(41) Salis, H. M.; Mirsky, E. A.; Voigt, C. A. Automated design of synthetic ribosome binding sites to control protein expression. *Nat. Biotechnol.* **2009**, *27*, 946−950.

(42) Shaner, N. C.; Campbell, R. E.; Steinbach, P. A.; Giepmans, B. N.; Palmer, A. E.; Tsien, R. Y. Improved monomeric red, orange and yellow fluorescent proteins derived from Discosoma sp. red fluorescent protein. *Nat. Biotechnol.* **2004**, *22*, 1567−1572.

(43) Pautot, S.; Frisken, B. J.; Weitz, D. A. Production of Unilamellar Vesicles Using an Inverted Emulsion. *Langmuir* **2003**, *19*, 2870−2879.

(44) Nishimura, K.; Hosoi, T.; Sunami, T.; Toyota, T.; Fujinami, M.; Oguma, K.; Matsuura, T.; Suzuki, H.; Yomo, T. Population analysis of structural properties of giant liposomes by flow cytometry. *Langmuir* **2009**, *25*, 10439−10443.

(45) Nishimura, K.; Matsuura, T.; Nishimura, K.; Sunami, T.; Suzuki, H.; Yomo, T. Cell-free protein synthesis inside giant unilamellar vesicles analyzed by flow cytometry. *Langmuir* **2012**, *28*, 8426−8432.

(46) Fujii, S.; Matsuura, T.; Sunami, T.; Kazuta, Y.; Yomo, T. In vitro evolution of alpha-hemolysin using a liposome display. *Proc. Natl. Acad. Sci. U. S. A.* **2013**, *110*, 16796−16801.

(47) Tso, J. Y.; Siebel, C. Cloning and expression of the phospholipase C gene from Clostridium perfringens and Clostridium bifermentans. *Infect. Immun.* **1989**, *57*, 468−476.

(48) Lim, H. J.; Park, Y. J.; Jang, Y. J.; Choi, J. E.; Oh, J. Y.; Park, J. H.; Song, J. K.; Kim, D. M. Cell-free synthesis of functional phospholipase A1 from Serratia sp. *Biotechnol. Biofuels* **2016**, *9*, 159.

(49) Haller, A.; Souliere, M. F.; Micura, R. The dynamic nature of RNA as key to understanding riboswitch mechanisms. *Acc. Chem. Res.* **2011**, *44*, 1339−1348.

(50) Peselis, A.; Serganov, A. Themes and variations in riboswitch structure and function. *Biochim. Biophys. Acta, Gene Regul. Mech.* **2014**, *1839*, 908−918.

(51) Fujii, S.; Matsuura, T.; Sunami, T.; Nishikawa, T.; Kazuta, Y.; Yomo, T. Liposome display for in vitro selection and evolution of membrane proteins. *Nat. Protoc.* **2014**, *9*, 1578−1591.

(52) Ausländer, D.; Eggerschwiler, B.; Kemmer, C.; Geering, B.; Ausländer, S.; Fussenegger, M. A designer cell-based histamine-specific human allergy profiler. *Nat. Commun.* **2014**, *5*, 4408.

(53) Nishimura, K.; Matsuura, T.; Sunami, T.; Fujii, S.; Nishimura, K.; Suzuki, H.; Yomo, T. Identification of giant unilamellar vesicles with permeability to small charged molecules. *RSC Adv.* **2014**, *4*, 35224−35232.

(54) Illangasekare, M.; Yarus, M. Phenylalanine-binding RNAs and genetic code evolution. *J. Mol. Evol.* **2002**, *54*, 298−311.

(55) Wilson, D. S.; Keefe, A. D. Random mutagenesis by PCR. *Curr. Protoc. Mol. Biol.* **2001**, *51*, 8.3.1−8.3.9.

(56) Dwidar, M.; Yokobayashi, Y. Controlling Bdellovibrio bacteriovorus Gene Expression and Predation Using Synthetic Riboswitches. *ACS Synth. Biol.* **2017**, *6*, 2035−2041.